

## Carbon-13 Chemical Shift Tensors of Disaccharides: Measurement, Computation and Assignment

Limin Shao,<sup>†</sup> Jonathan R. Yates,<sup>‡</sup> and Jeremy J. Titman<sup>\*,†</sup>

School of Chemistry, University of Nottingham, University Park, Nottingham, NG7 2RD, UK, and Cavendish Laboratory, University of Cambridge, 19 J. J. Thomson Avenue, Cambridge, CB3 0HE, UK

Received: July 26, 2007; In Final Form: September 17, 2007

A recently developed chemical shift anisotropy amplification solid-state nuclear magnetic resonance (NMR) experiment is applied to the measurement of the chemical shift tensors in three disaccharides: sucrose, maltose, and trehalose. The measured tensor principal values are compared with those calculated from first principles using density functional theory within the planewave–pseudopotential approach. In addition, a method of assigning poorly dispersed NMR spectra, based on comparing experimental and calculated shift anisotropies as well as isotropic shifts, is demonstrated.

### Introduction

Carbohydrates and oligosaccharides are essential biological molecules which function as metabolic energy sources, participate in cell signaling processes, and serve as structural components. Since crystalline samples are not always available for structural studies, solid-state nuclear magnetic resonance (NMR) provides a useful complement to diffraction techniques. For example, early cross polarization magic angle spinning (CPMAS) studies clarified the morphology of cellulose<sup>1,2</sup> and starches.<sup>3</sup> Later investigations demonstrated that the isotropic carbon-13 shifts of glycosidic carbon atoms are correlated with the torsion angles that describe the conformation of the glycosidic linkage.<sup>4,5</sup> This observation allowed studies of crystallization and polymorphism,<sup>6,7</sup> as well as aggregation and gelation<sup>8</sup> in starch, and more recently, a detailed investigation of conformational distributions in glassy trehalose.<sup>9</sup>

In principle, the full chemical shift tensor can provide more information about the local structure than its isotropic average. For example, it has been shown recently that the carbon-13 chemical shift tensors for the anomeric site in the  $\alpha$  form of monosaccharides are generally more axially symmetric than those in the  $\beta$  anomer.<sup>10</sup> Measurements of the chemical shift tensor can be made directly from wide-line spectra of powders which show singularities corresponding to the principal components. However, this approach suffers from poor sensitivity, interference from weak homonuclear dipolar couplings, and spectral overlap in samples with many chemical sites. Hence, it has become routine to resort instead to analysis<sup>11</sup> of the intensities of the rotational sidebands<sup>12</sup> which appear in the MAS spectrum. A relatively low MAS rate is often required to give sufficient sidebands, especially when the anisotropy is small, and this results in loss of resolution due to the overlap of different sideband manifolds. Hence, a large number of two-dimensional experiments have been designed that separate the MAS sideband manifolds in crowded spectra according to their isotropic shifts. However, for saccharides, poor shift dispersion, small anisotropies, and long spin–lattice relaxation times combine to constitute a significant challenge for these methods,

and few measurements of chemical shift tensors in carbohydrates and oligosaccharides have been reported.

In this paper, we apply a recently developed chemical shift anisotropy (CSA) amplification experiment<sup>13,14</sup> to the measurement of the chemical shift tensors in three disaccharides: glucose, maltose, and trehalose. With CSA amplification, the standard MAS spectrum in one dimension is correlated with a sideband pattern in the other in which the intensities reflect those expected for a sample spinning at some fraction,  $1/x_a$ , of the actual rate,  $\omega_r$ .<sup>15</sup> Hence, such methods are particularly useful for measuring small anisotropies for which prohibitively low MAS rates would otherwise be required to give sufficient sidebands for analysis. In addition, we compare the chemical shift tensors measured by CSA amplification with those calculated from first principles using density functional theory within the planewave–pseudopotential approach<sup>16,17</sup> and the gauge including projector-augmented wave (GIPAW) method.<sup>18</sup>

The poor dispersion observed in carbon-13 MAS spectra of carbohydrates and oligosaccharides makes assignments difficult. It should be noted that the reduction in conformational flexibility for solid saccharides often results in significant differences between solution-state and MAS isotropic shifts, such that a straightforward comparison does not constitute an assignment strategy. In a unique example, Sherwood et al.<sup>19</sup> resorted to a single-crystal sample of sucrose and used the additional information present about tensor orientations to make a systematic assignment based on local molecular symmetry considerations. In principle, comparisons between isotropic chemical shifts measured with MAS and calculated values provide a more straightforward means of assigning solid-state carbon-13 spectra. In practice, the poor shift dispersion makes this process less than reliable, since pairs of resonances are often within the root-mean-square deviation between the calculated and experimental values. Yates et al.<sup>20</sup> used the correlation between carbon-13 and proton isotropic shifts obtained from a two-dimensional MAS-J-HMQC spectrum<sup>21</sup> to distinguish between poorly dispersed experimental and calculated values in maltose. In this paper, we investigate an alternative approach; namely, that the correlation between the isotropic chemical shift and the shift anisotropy can be used as a comparable aid to assignment in poorly dispersed spectra.

<sup>†</sup> University of Nottingham.

<sup>‡</sup> University of Cambridge.

## Experimental and Computational Section

**Disaccharide Samples.** Samples described by the manufacturers as D-maltose monohydrate (98%),  $\alpha,\alpha$ -D-trehalose (99%), and sucrose (98%) were purchased from Sigma-Aldrich and Acros Organics and used without further purification. Sucrose and  $\alpha,\alpha$ -D-trehalose are single anomers, more systematically designated  $\alpha$ -D-glucopyranosyl- $\beta$ -D-fructofuranoside and  $\alpha$ -D-glucopyranosyl- $\alpha$ -D-glucopyranoside, respectively. D-Maltose, on the other hand, is potentially a mixture of the two anomers of 4-O- $\alpha$ -D-glucopyranosyl-D-glucopyranoside.

**Solid-State NMR Measurements.** Carbon-13 NMR spectra were recorded at a Larmor frequency of 75.47 MHz on samples of disaccharides packed into 4 mm rotors spinning in a double-resonance MAS probe. Standard CPMAS spectra were obtained by co-adding between 32 and 256 scans with a spectral width of 27.278 kHz. The MAS rate was 4.8 kHz, stabilized to  $\pm 5$  Hz, resulting in sideband-free spectra. Proton decoupling at a field strength of 85 kHz was applied during the acquisition time, which was 75 ms in duration. The contact time and the relaxation delay were optimized for each sample and ranged between 2.5 and 3.5 ms and 50 and 55 s. Isotropic carbon-13 chemical shifts were referenced externally to the high-frequency carbon-13 line of solid adamantane, which in turn was assigned a shift of 37.8 ppm relative to the carbon in TMS.

Carbon-13 CSA amplification spectra were recorded as described in ref 14 using two sequences of five  $\pi$  pulses with timings chosen to achieve an amplification factor of 8. Two experiments were recorded for each sample with MAS rates of 4 and 4.8 kHz, resulting in effective rates of 500 and 600 Hz in the  $\omega_1$  dimension. Heteronuclear decoupling was interrupted during the  $\pi$  pulses to avoid unwanted Hartmann–Hahn contacts, and the delays between them were reduced to take account of their finite length. The effects of experimental imperfections and resonance offsets were reduced by shifting the relative phases of successive  $\pi$  pulses through the series  $0^\circ, 330^\circ, 60^\circ, 330^\circ, 0$ . There were 16 values of  $t_1$  with an increment corresponding to 1/16 of the MAS period, and typically 256 scans were acquired for each increment. The carbon-13  $\pi$  pulse was 5  $\mu$ s. Other experimental parameters were identical to those used for standard CPMAS spectra, as described above.

Sideband intensities were extracted from the  $\omega_1$  dimension of CSA amplification experiments. The chemical shift anisotropy,  $\zeta$ , and asymmetry,  $\eta$ , were extracted using a least-squares fitting procedure. This involves comparing the experimental sideband intensities to those simulated for a standard MAS spectrum at the effective MAS rate using the SIMPSON program.<sup>22</sup> The principal components of the chemical shift tensor  $\delta_{XX}, \delta_{YY}$  and  $\delta_{ZZ}$ , ordered such that  $|\delta_{ZZ} - \delta_{iso}| \geq |\delta_{XX} - \delta_{iso}| \geq |\delta_{YY} - \delta_{iso}|$ , were then calculated according to the definitions  $\zeta = \delta_{ZZ} - \delta_{iso}$  and  $\eta = (\delta_{YY} - \delta_{XX})/\zeta$ . The variation of the extracted  $\zeta$  and  $\eta$  obtained by employing an increasing number of crystallite orientations for powder averaging was investigated to ensure convergence to within an acceptable margin of error. The values quoted here were obtained using 31 ( $\alpha, \beta$ ) crystallite orientations distributed over an octant according to a Lebedev scheme.<sup>23</sup> As a check of reproducibility, principal components obtained from two CSA amplification experiments recorded with effective MAS rates  $\omega_r/x_a$  of 500 and 600 Hz were compared. The root-mean-square deviation (rmsd) between the two datasets varied from 0.9 ppm for  $\alpha,\alpha$ -D-trehalose to 1.5 ppm for  $\beta$ -D-maltose.

**First-Principles Calculations.** First-principles calculations were performed with the density functional code CASTEP,<sup>16</sup>

which uses a planewave basis to expand the charge density and the electronic wavefunctions and employs pseudopotentials to represent the core electrons. All calculations used the PBE<sup>24</sup> exchange-correlation functional. The initial geometry optimization employed Vanderbilt's "Ultrasoft" pseudopotentials<sup>25</sup> and a maximum planewave energy of 30 Ryd. NMR parameters were calculated with the GIPAW method<sup>18</sup> using Troullier–Martins norm-conserving pseudopotentials<sup>26</sup> and planewaves up to a maximum energy of 80 Ryd. The output of the calculation is the absolute shielding tensor,  $\sigma$ , defined as the ratio between a uniform external magnetic field,  $\mathbf{B}_0$ , and the induced magnetic field,  $\mathbf{B}_{in}$ ,

$$\mathbf{B}_{in} = -\sigma\mathbf{B}_0$$

The principal components of the shielding tensor were obtained by diagonalizing the symmetric part, and their isotropic average was calculated from

$$\sigma_{iso} = \frac{1}{3}(\sigma_{XX} + \sigma_{YY} + \sigma_{ZZ})$$

Chemical shifts are measured relative to a reference frequency such that their direction is the opposite of the shielding. Hence, the isotropic chemical shift was obtained from the isotropic average of the shielding tensor according to

$$\delta_{iso} = -[\sigma_{iso} - \sigma_{ref}]$$

where for  $^{13}\text{C}$  we use  $\sigma_{ref} = 168.1$  ppm taken from earlier work.<sup>20</sup> The principal components of the chemical shift tensor were calculated from those of the shielding tensor in a similar fashion.

The crystal structures of sucrose<sup>27</sup> and  $\beta$ -D-maltose monohydrate<sup>28</sup> determined by neutron diffraction, as well as that of  $\alpha,\alpha$ -D-trehalose<sup>29</sup> obtained by X-ray diffraction, were taken from the Cambridge Crystallographic database.<sup>30</sup> Positions of hydrogen atoms determined by X-ray diffraction are known to be less accurate than those obtained by neutron diffraction. Hence, for consistency, partial geometry optimizations were performed on all three structures, allowing only the positions of the hydrogen atoms to move. Note that for sucrose, two X-ray structures are also available,<sup>31,32</sup> but after optimization of the hydrogen positions, both of these were found to give shielding tensors in close agreement with those calculated from the neutron structure.

## Results and Discussion

**CPMAS Spectra and Carbon-13 Isotropic Shifts.** Figure 1 shows standard carbon-13 CPMAS spectra of the three disaccharides studied, recorded as described above. The range of isotropic carbon-13 chemical shifts is relatively small, and the resonances can be divided into three groups. Anomeric carbons result in resonances between 90 and 110 ppm, whereas those below 70 ppm generally correspond to primary alcohol carbons. The remaining pyranose ring carbon sites appear in a narrow range between  $\sim 70$  and 85 ppm, with the least shift dispersion evident for  $\alpha,\alpha$ -D-trehalose due to the approximate  $C_2$  molecular symmetry evident from the crystal structure.<sup>29</sup> Because the CSAs of all carbon sites in saccharides are relatively small, there were no significant spinning sidebands in the CPMAS spectra of any of the samples at this MAS rate.

The carbon-13 CPMAS spectrum of sucrose can be assigned following the single-crystal studies of Sherwood et al.; however, although the latter study found a difference of 0.5 ppm between

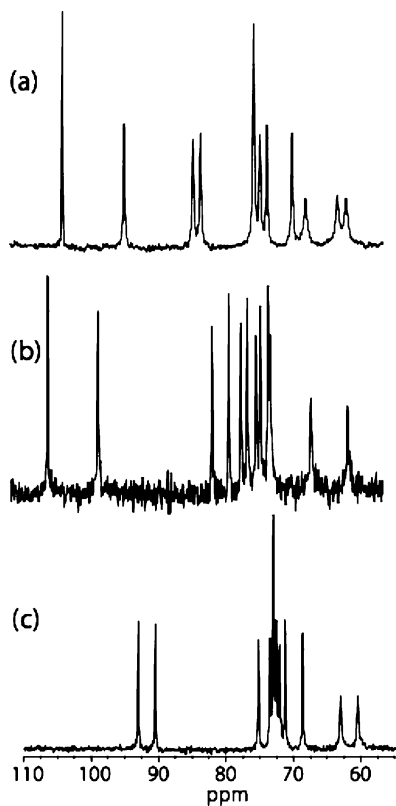


**Figure 1.** Carbon-13 CPMAS spectra of (a) D-sucrose, (b) D-maltose monohydrate, and (c)  $\alpha,\alpha$ -D-trehalose recorded using parameters described in the text.

them, the C2 and C5 resonances are not resolved in Figure 1a. For D-maltose monohydrate, the carbon-13 CPMAS spectrum of Figure 1b shows the expected 12 peaks, and a comparison with isotropic chemical shifts calculated by Yates et al.<sup>20</sup> indicates that this sample contains only the  $\beta$ -anomer, 4-*O*- $\alpha$ -D-glucopyranosyl- $\beta$ -D-glucopyranoside. For  $\alpha,\alpha$ -D-trehalose, 11 peaks are observed in the carbon-13 CPMAS spectrum of Figure 1c, suggesting one unresolved pair of lines. A similar spectrum, albeit with somewhat lower resolution, was reported by Jeffrey and Nanni.<sup>29</sup> These authors were unable to rationalize the differences in chemical shift between the two anomeric carbon sites with the approximate  $C_2$  molecular symmetry found by X-ray crystallography and reported no assignments other than a tentative association of C4 with a peak at 78 ppm. As shown below, the combination of CSA amplification measurements and first principles calculations of the carbon-13 chemical shift anisotropy provides a method to assign the majority of the carbon-13 resonances in  $\alpha,\alpha$ -D-trehalose.

**CSA Amplification Spectra and Carbon-13 Chemical Shift Tensors.** Figure 2, which shows the carbon-13 CSA amplification spectrum of sucrose, recorded as described above, illustrates the application of this method to disaccharides. Because the MAS rate is relatively high, no spinning sidebands appear in the  $\omega_2$  dimension so that the carbon-13 sites can be resolved by their isotropic shifts, as in the standard CPMAS spectrum of Figure 1a. However, there are at least seven significant spinning sidebands for each carbon-13 site in  $\omega_1$ , for which the effective MAS rate is 500 Hz. The principal values of the carbon-13 chemical shift tensors of sucrose were first measured by Sherwood et al.<sup>19</sup> using a two-dimensional experiment that correlates the chemical shifts observed in a single-crystal sample for two orientations related via a mechanical flip. More recently, Witter et al.<sup>33</sup> studied a powdered sample with a modified version of an experiment due to Tycko et al.<sup>34</sup> in which a

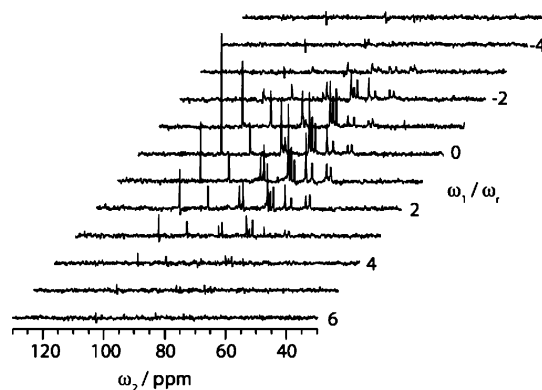


**Figure 2.** Carbon-13 CSA amplification spectrum of sucrose, recorded as described in the text, using a MAS rate of 4 kHz.

multiple-pulse sequence operating during the evolution period interferes with the MAS averaging and reintroduces a scaled CSA powder pattern. Table 1 shows a comparison between the principal components of the carbon-13 chemical shift tensors obtained in this work using CSA amplification and those reported in refs 19 and 33, with the assignment taken from Sherwood et al. Table 2 shows a similar comparison in terms of the tensor parameters anisotropy,  $\zeta$ , and asymmetry,  $\eta$ .

The rmsd between the two previous measurements is 4.5 ppm, falling to 4.2 ppm if the values for C2 and C5 are omitted. In the two-dimensional spectrum recorded by Witter et al. for a powdered sample, these two lines are not sufficiently resolved to allow the complete separation of the corresponding powder patterns. The principal components quoted by Witter et al. for C5 deviate by as much as 10.4 ppm from those given by Sherwood et al. There is a similar problem of overlap in the carbon-13 CSA spectrum of Figure 2, and so principal components for C5 have not been obtained in this work. The rmsd between the results obtained in this work and those of Sherwood et al. is only 3.0 ppm, indicating that the CSA amplification measurements of this work are in better agreement with the single-crystal data than the measurements of Witter et al. It should be noted that the principal components measured by CSA amplification generally fall between those reported in refs 19 and 33. Similarly, the anisotropy obtained from the single crystal measurements of Sherwood et al. always has the largest magnitude, whereas with one exception, that obtained by Witter et al. has the smallest. These observations suggest small systematic errors in at least two, if not all, of the measurements of  $\zeta$ . For the asymmetry, although the differences between the measurements are substantial, no systematic trends can be identified. It should be noted that the effective MAS rate  $\omega_r/x_a$  was chosen so that there are roughly seven significant sidebands in the  $\omega_1$  dimension of the CSA amplification spectra. Recently, Hodgkinson and Emsley<sup>35</sup> investigated the reliability of the CSA parameters determined in this way by calculating their minimum variance bounds. Their somewhat surprising conclusion is that measurements of  $\zeta$  made from a moderate number of MAS sidebands are generally more reliable than those from the wide-line spectrum, whereas reliable determinations of  $\eta$  require more sidebands. Hence, the choice of  $\omega_r/x_a$  made here optimizes the reliability of the extracted  $\zeta$  at the expense of the accuracy of  $\eta$ .

For sucrose, all three measurements show consistently that the primary alcohol carbon sites (C6, C6', and C1') have relatively large and negative  $\zeta$ , but the two anomeric carbon sites have very different anisotropies, despite their similar  $\delta_{iso}$  values. To our knowledge, there are no previous measurements of the chemical shift tensors of the other two disaccharides.

**TABLE 1: Comparison of Principal Components of Carbon-13 Chemical Shift Tensors<sup>a</sup> of Sucrose Obtained in This Work with Those Measured Previously**

carbon site <sup>b</sup>	this work			Witter et al <sup>33</sup>			Sherwood et al <sup>19</sup>		
	$\delta_{XX}$	$\delta_{YY}$	$\delta_{ZZ}$	$\delta_{XX}$	$\delta_{YY}$	$\delta_{ZZ}$	$\delta_{XX}$	$\delta_{YY}$	$\delta_{ZZ}$
C2'	88.3	101.4	118.4	92.8	100.5	114.7	89.9	97.7	120.6
C1	72.2	91.3	117.3	74.4	90.8	115.3	69.1	89.1	123.8
C3'	68.3	80.1	100.9	70.5	79.2	99.3	68.5	77.4	104.1
C5'	102.1	90.2	53.7	100.6	90.6	54.8	105.5	92.2	48.4
C2 <sup>c</sup>	93.3	76.6	52.0	90.5	77.1	54.6	94.2	74.5	53.6
C5 <sup>c</sup>				90.3 <sup>d</sup>	75.9 <sup>d</sup>	54.6 <sup>d</sup>	93.7	82.8	44.2
C3	91.3	73.7	54.0	88.7	73.2	56.7	91.8	73.3	53.6
C4'	49.2	69.0	97.8	51.3	67.6	97.1	46.7	66.1	103.6
C4	84.7	76.2	43.7	84.0	73.1	47.0	86.0	77.1	40.7
C1'	85.6	71.0	42.0	86.4	72.1	40.7	87.1	74.4	38.0
C6'	81.7	68.6	33.9	82.2	67.4	34.5	84.3	69.8	29.8
C6	82.7	66.3	31.3	79.5	66.7	34.7	86.3	67.2	28.1

<sup>a</sup> In parts per million. <sup>b</sup> Assigned according to ref 19. <sup>c</sup> These sites cannot be resolved in this work. <sup>d</sup> Erroneous due to overlap with C2.

**TABLE 2: Comparison of Carbon-13 Chemical Shift Tensor Parameters<sup>a</sup> of D-Sucrose Obtained in This Work with Those Measured Previously**

carbon site <sup>b</sup>	this work			Witter et al <sup>33</sup>			Sherwood et al <sup>19</sup>		
	$\delta_{iso}$	$\zeta$	$\eta$	$\delta_{iso}$	$\zeta$	$\eta$	$\delta_{iso}$	$\zeta$	$\eta$
C2'	102.7	15.7	0.84	102.7	12.0	0.64	102.7	17.9	0.44
C1	93.6	23.7	0.80	93.5	21.8	0.75	94.0	29.8	0.67
C3'	83.1	17.8	0.66	83.0	16.3	0.53	83.3	20.8	0.43
C5'	82.0	-28.3	0.42	82.0	-27.2	0.37	82.0	-33.6	0.40
C2 <sup>c</sup>	74.0	-22.0	0.76	74.1	-19.5	0.69	74.1	-20.5	0.96
C5 <sup>c</sup>				73.6	-19.0 <sup>d</sup>	0.76 <sup>d</sup>	73.6	-29.4	0.37
C3	73.0	-19.0	0.93	72.9	-16.2	0.96	72.9	-19.3	0.96
C4'	72.0	25.8	0.77	72.0	25.1	0.65	72.1	31.5	0.62
C4	68.2	-24.5	0.35	68.0	-21.0	0.52	67.9	-27.2	0.33
C1'	66.2	-24.2	0.60	66.4	-25.7	0.56	66.5	-28.5	0.45
C6'	61.4	-27.5	0.48	61.4	-26.9	0.55	61.3	-31.5	0.46
C6	60.1	-28.8	0.57	60.3	-25.6	0.50	60.5	-32.4	0.59

<sup>a</sup>  $\delta_{iso}$  and  $\zeta$  in parts per million. <sup>b</sup> Assigned according to ref 19. <sup>c</sup> These sites cannot be resolved in this work. <sup>d</sup> Erroneous due to overlap with C2.

**TABLE 3: Experimental Principal Components of Carbon-13 Chemical Shift Tensors and Tensor Parameters<sup>a</sup> for  $\beta$ -D-Maltose Monohydrate**

carbon site <sup>b</sup>	$\delta_{XX}$	$\delta_{YY}$	$\delta_{ZZ}$	$\delta_{iso}$	$\zeta$	$\eta$
C1	87.5	103.1	122.9	104.5	18.4	0.85
C1'	114.6	100.8	75.5	97.0	-21.5	0.65
C4'	101.9	97.2	41.4	80.2	-38.8	0.12
C2'	88.9	78.0	66.2	77.7	-11.5	0.96
C5'	91.8	85.5	50.5	75.9	-25.4	0.25
C3'	58.7	75.0	91.3	75.0	16.3	1.00
C3	59.5	71.1	90.5	73.7	16.8	0.70
C4	89.9	74.6	54.8	73.1	-18.3	0.84
C5	91.1	74.8	49.9	71.9	-22.0	0.74
C2	86.8	77.0	51.0	71.6	-20.6	0.48
C6	87.0	69.5	40.2	65.6	-25.4	0.69
C6'	81.8	66.8	32.0	60.2	-28.2	0.53

<sup>a</sup> In parts per million, except  $\eta$ . <sup>b</sup> Assigned according to ref 20.

Tables 3 and 4 show the principal components of the carbon-13 chemical shift tensors obtained using CSA amplification for  $\beta$ -D-maltose monohydrate and  $\alpha,\alpha$ -D-trehalose, respectively. Assignments have been made by a comparison with calculated values, as described below. For  $\beta$ -D-maltose monohydrate, the anisotropies are, on average, smaller than for similar sites in sucrose. Once again, primary alcohol carbon sites (C6, C6') have the largest magnitude for  $\zeta$ , except for the glycosidic C4 carbon. For  $\alpha,\alpha$ -D-trehalose, the approximate  $C_2$  molecular symmetry results in many similarities between the chemical shift tensors at equivalent sites in the two rings. For example, the two anomeric carbon sites have  $\zeta$  and  $\eta$  much closer to one another than in either sucrose or  $\beta$ -D-maltose monohydrate.

**TABLE 4: Experimental Principal Components of Carbon-13 Chemical Shift Tensors and Tensor Parameters<sup>a</sup> for  $\alpha,\alpha$ -D-Trehalose**

carbon site <sup>b</sup>	$\delta_{XX}$	$\delta_{YY}$	$\delta_{ZZ}$	$\delta_{iso}$	$\zeta$	$\eta$
C1'	73.5	91.2	114.6	93.1	21.5	0.82
C1	69.8	88.3	113.4	90.5	22.9	0.81
C3	63.6	74.4	87.9	75.3	12.6	0.85
C4	87.9	76.0	56.9	73.6	-16.7	0.72
C5 <sup>c</sup> , C2' <sup>c</sup>	56.3	73.1	89.9	73.1	16.8	0.82
C2	56.3	71.6	90.2	72.7	17.5	0.88
C3'	56.2	70.9	89.4	72.2	17.2	0.85
C5'	90.6	75.0	48.6	71.4	-22.8	0.69
C4'	87.0	75.2	44.2	68.8	-24.6	0.48
C6	85.5	66.2	37.9	63.2	-25.3	0.77
C6'	82.9	64.6	34.6	60.7	-26.1	0.70

<sup>a</sup> In parts per million, except  $\eta$ . <sup>b</sup> Assigned in this work by comparison with calculations. <sup>c</sup> These sites cannot be resolved in this work.

**Calculated Carbon-13 Chemical Shift Tensors of Disaccharides.** Principal components of the carbon-13 chemical shift tensors of sucrose,  $\beta$ -D-maltose monohydrate and  $\alpha,\alpha$ -D-trehalose, calculated according to the procedures described above are shown in Tables 5–7. Agreement between experimental and calculated isotropic shifts is very good, with the rmsd ranging from 1.5 ppm for sucrose to 1.1 ppm for  $\alpha,\alpha$ -D-trehalose. However, the density functionals used in the calculations are known to overestimate the paramagnetic contribution to the shielding,<sup>20</sup> which results in erroneously large calculated isotropic shifts for anomeric carbon sites and erroneously small ones for primary alcohol carbons. When these two groups of resonances are omitted, the agreement is better, with the rmsd

**TABLE 5: Calculated Principal Components of Carbon-13 Chemical Shift Tensors and Tensor Parameters<sup>a</sup> for Sucrose**

carbon site	$\delta_{XX}$	$\delta_{YY}$	$\delta_{ZZ}$	$\delta_{iso}$	$\zeta$	$\eta$
C2'	89.23	97.98	125.24	104.15	21.09	0.41
C1	66.37	88.38	127.39	94.05	33.34	0.66
C3'	66.95	76.06	106.97	83.33	23.65	0.39
C5'	105.41	94.73	45.59	81.91	-36.32	0.29
C2	50.39	72.05	96.08	72.84	23.24	0.93
C5	96.30	80.63	41.56	72.83	-31.27	0.50
C3	94.55	71.71	47.87	71.38	-23.50	0.97
C4'	42.03	64.46	104.43	70.31	34.12	0.66
C4	86.79	77.48	35.05	66.44	-31.39	0.30
C1'	88.22	70.62	32.97	63.93	-30.97	0.57
C6'	85.69	69.68	22.81	59.39	-36.58	0.44
C6	88.42	66.10	21.07	58.53	-37.46	0.60

<sup>a</sup> In parts per million, except  $\eta$ .**TABLE 6: Calculated Principal Components of Carbon-13 Chemical Shift Tensors and Tensor Parameters<sup>a</sup> for  $\beta$ -D-Maltose Monohydrate**

carbon site	$\delta_{XX}$	$\delta_{YY}$	$\delta_{ZZ}$	$\delta_{iso}$	$\zeta$	$\eta$
C1	87.55	105.97	127.48	107.00	20.48	0.90
C1'	123.86	102.34	71.70	99.30	-27.60	0.78
C4'	105.57	101.33	33.64	80.18	-46.54	0.09
C2'	90.43	79.81	62.23	77.49	-15.26	0.70
C5'	94.80	86.43	45.99	75.74	-29.75	0.28
C3'	55.23	74.08	95.75	75.02	20.73	0.91
C3	55.84	67.41	94.07	72.44	21.63	0.53
C4	91.86	76.64	48.76	72.42	-23.66	0.64
C5	96.37	73.76	44.76	71.63	-26.87	0.84
C2	89.18	78.01	47.40	71.53	-24.13	0.46
C6	93.93	68.57	30.01	64.17	-34.16	0.74
C6'	86.09	66.95	23.09	58.71	-35.62	0.54

<sup>a</sup> In parts per million, except  $\eta$ .**TABLE 7: Calculated Principal Components of Carbon-13 Chemical Shift Tensors and Tensor Parameters<sup>a</sup> for  $\alpha,\alpha$ -D-Trehalose**

carbon site	$\delta_{XX}$	$\delta_{YY}$	$\delta_{ZZ}$	$\delta_{iso}$	$\zeta$	$\eta$
C1'	69.23	92.36	125.26	95.62	29.65	0.78
C1	68.31	87.42	122.91	92.88	30.03	0.64
C3	61.10	75.41	90.27	75.59	14.67	0.98
C4	92.31	79.01	50.60	73.98	-23.37	0.57
C5	50.82	72.77	95.75	73.11	22.64	0.97
C2'	52.41	71.31	94.58	72.77	21.81	0.87
C2	53.13	70.91	93.06	72.37	20.70	0.86
C3'	49.79	71.06	93.32	71.39	21.93	0.97
C5'	96.77	79.05	41.88	72.57	-30.69	0.58
C4'	89.58	80.16	35.10	68.28	-33.18	0.28
C6	90.95	68.69	27.77	62.47	-34.70	0.64
C6'	89.48	66.86	25.01	60.45	-35.44	0.64

<sup>a</sup> In parts per million, except  $\eta$ .

falling to 1.3 ppm for sucrose and only 0.5 ppm for  $\alpha,\alpha$ -D-trehalose. The comparison between the experimental and calculated isotropic shifts for  $\beta$ -D-maltose monohydrate has been discussed previously.<sup>20</sup> For sucrose, the calculated isotropic shifts confirm the assignments of Sherwood et al., whereas for  $\alpha,\alpha$ -D-trehalose, the comparison between experiment and calculation allows the two anomeric carbon sites (C1 and C1') and the two primary alcohol sites (C6 and C6') to be clearly distinguished in contrast to ref 29. The former observation is particularly interesting in light of the crystal structure,<sup>29</sup> which shows only small conformational differences between the two rings in the vicinity of the glycosidic linkage. For example, the two glycosidic torsion angles are almost identical at  $+60.8^\circ$  and  $+60.1^\circ$ . This suggests that MAS chemical shifts are sensitive to the combination of these small conformational differences and longer-range crystal packing effects. The most significant

difference between the two rings is the conformation around the C5-C6 and C5'-C6' bonds, for which the O-C-C-O torsion angles are  $-72^\circ$  and  $+71^\circ$ , respectively. This results in a substantially shielded  $\delta_{ZZ}$  for C4', with the primary alcohol hydroxyl group gauche relative to C4 with it trans, and a change in the sign of  $\zeta$  for C5 and C5'. The former is an example of the well-known gamma gauche effect.<sup>36</sup>

Despite the good agreement observed for their isotropic average, comparison between experimental and calculated tensor components indicates that the magnitude of the calculated  $\zeta$  is consistently too large. This suggests that the overestimation of the paramagnetic shielding mentioned above results in the over- and underestimation of the maximum and minimum principal components of the shift, respectively. Previous authors have proposed several schemes to empirically adjust the paramagnetic component.<sup>37,38</sup> Hence, in this work, to facilitate comparison with experiment, the calculated tensor width (defined as the difference  $\delta_{ZZ} - \delta_{XX}$ , and sometimes denoted the "span") was scaled by a constant factor for each disaccharide so as to minimize the rmsd between calculated and experimental principal values. The values of the isotropic shift and the asymmetry were not adjusted during this scaling procedure. It should be noted that an alternative scaling procedure that involved minimizing the magnitude of the anisotropy was also tested and gave very similar results.

For sucrose, scaling the calculated width by 0.77 resulted in a rmsd of 2.1 ppm from the principal values measured by CSA amplification, whereas a scaling factor of 0.88 gave a similar rmsd of 1.8 ppm from the single-crystal data of Sherwood et al.<sup>19</sup> Scaling factors of 0.80 and 0.76 were required for  $\beta$ -D-maltose monohydrate and  $\alpha,\alpha$ -D-trehalose, giving an rmsd from the CSA amplification measurements of 1.7 ppm in both cases. Figure 3 shows plots of the anisotropy determined from the scaled principal components against the calculated isotropic shift, superimposed on a similar plot of the experimental values for (a) sucrose, (b)  $\beta$ -D-maltose monohydrate, and (c)  $\alpha,\alpha$ -D-trehalose. The agreement between the experimental data and the scaled calculations is very good. The one exception is the sucrose C2 site for which the calculated anisotropy is of opposite sign to the CSA amplification value to that reported by Sherwood et al. However, this site has  $\eta$  close to unity where the sign of the anisotropy is poorly defined. The overestimation of the tensor widths shows remarkably little variation among the three disaccharides and is somewhat larger than found for other materials using the same level of theory; for example, a scaling of 0.95 was observed previously for several amino acids.<sup>39</sup> Reproducing the tensor widths without scaling is clearly desirable and will form an important test in the development of new exchange-correlation functionals.

**Assignment.** The lack of dispersion in the spectra of Figure 1 suggests that a comparison between calculated and experimental isotropic shifts will not be sufficient to definitively assign the carbon-13 resonances of the disaccharides. Indeed, the difference between adjacent isotropic chemical shifts is often less than the rmsd between the calculated and the experimental data. However, the anisotropy provides a further convenient parameter that can be used to distinguish between assignments in cases of ambiguity, and the plots of Figure 3 represent the correlation between  $\delta_{iso}$  and  $\zeta$  in a convenient fashion.

Of the 12 carbon-13 resonances in sucrose, four (C2', C1, C4, and C1') can be confidently assigned on the basis of the agreement between the calculated and experimental isotropic shifts. The sign of the anisotropy alone is sufficient to distinguish between the pairs C3'/C5' and C3/C4', for which the isotropic

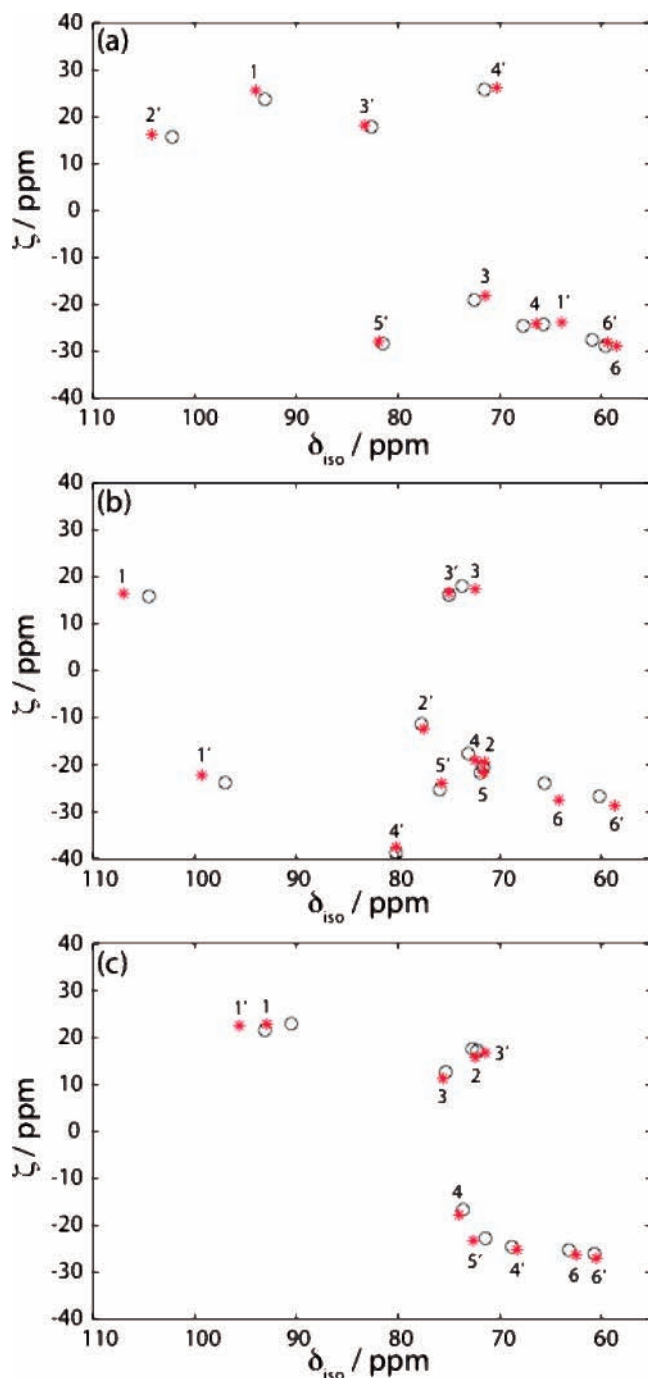


**Figure 3.** Plots of the shift anisotropy,  $\zeta$ , against the isotropic shift (circles) measured using CSA amplification and (asterisks) calculated and scaled for (a) sucrose, omitting C2 and C5; (b)  $\beta$ -D-maltose monohydrate; and (c)  $\alpha,\alpha$ -D-trehalose, omitting C5 and C2'. The calculated points are labeled according to the carbon site.

shifts are within 1 ppm. Sites C6 and C6' differ by just 1.3 and 1.2 ppm in  $\delta_{\text{iso}}$  and  $\zeta$ , respectively, but the correlation between these two parameters clearly supports the assignment of Sherwood et al., and the good agreement between calculated and experimental asymmetries provides further confirmation. C2 and C5 could not be distinguished in this work due to overlap in the one-dimensional MAS spectrum. Hence, the correlation between  $\delta_{\text{iso}}$  and  $\zeta$  in Figure 3a leads to the same assignment for the carbon-13 resonance of sucrose as in ref 19.

Of the 12 carbon-13 resonances in maltose, six (C1, C1', C4', C2', C6 and C6') can be assigned by consideration of the isotropic shifts alone, whereas the poorly dispersed pairs C3'/C5' and C3/C4 can be resolved by the contrasting signs of their

anisotropies. C2 and C5, were only tentatively assigned in ref 20, but the correlation between  $\delta_{\text{iso}}$  and  $\zeta$  in Figure 3b and the good agreement between the experimental and calculated  $\eta$  support that assignment. Hence, the correlation between  $\delta_{\text{iso}}$  and  $\zeta$  in Figure 3b confirms the assignment of maltose due to Yates et al.

For  $\alpha,\alpha$ -trehalose, there is no previous assignment, and indeed, Jeffrey and Nanni<sup>29</sup> were unable to explain the difference in isotropic shift between the two anomeric carbons (C1 and C1'), given the approximate  $C_2$  molecular symmetry. Nevertheless, the calculations performed here which are based on the crystal structure of ref 29 do separate the isotropic shifts of these two sites by nearly 3 ppm and the two primary alcohol carbons (C6 and C6') by 2 ppm. Six resonances fall between 74 and 71 ppm, but there are two additional well-resolved peaks which can be assigned to C3 at 75.3 ppm and C4' at 68.8 ppm. Hence, six resonances can be assigned by a comparison between experimental and calculated isotropic shifts alone. It should be noted that the small, positive  $\zeta$  observed for C3 and the corresponding large, negative value for C4' are also obtained by calculation, and this confirms the assignment. It should be noted that Jeffrey and Nanni tentatively assigned the C3 resonance to C4, but consideration of the sign of the anisotropy suggests this is incorrect. Of the six remaining peaks, four have positive  $\zeta$ , while C4 and C5' can be distinguished by their negative values. It should be noted that this suggests that the experimental  $\delta_{\text{iso}}$  for C3' is larger than for C5', in contrast to the calculations. C2 and C3' have been tentatively assigned on the grounds of their  $\eta$  values.

## Conclusion

The utility of the chemical shift anisotropy amplification experiment for measuring NMR chemical shift tensors with small anisotropies has been illustrated using three disaccharides as examples. The ability of first principles calculations using density functional theory within the planewave-pseudopotential approach to accurately reproduce the experimental principal components has also been demonstrated. A method of assigning poorly dispersed NMR spectra on the basis of comparing experimental and calculated shift anisotropies as well as isotropic shifts has also been described.

**Acknowledgment.** The authors thank Dr. S. P. Brown (Warwick) for helpful discussions. L.S. and J.J.T. acknowledge financial support from EPSRC Grant EP/E003052. J.R.Y. thanks Corpus Christi College, Cambridge for a Research Fellowship.

## References and Notes

- (1) Atalla, R. H.; Gast, J. C.; Sindorf, D. W.; Bartuska, V. J.; Maciel, G. E. *J. Am. Chem. Soc.* **1980**, *102*, 3249.
- (2) Earl, W. L.; VanderHart, D. L. *J. Am. Chem. Soc.* **1980**, *102*, 3251.
- (3) Gidley, M. J.; Bociek, S. M. *J. Am. Chem. Soc.* **1985**, *107*, 7040.
- (4) Gidley, M. J.; Bociek, S. M. *J. Am. Chem. Soc.* **1988**, *110*, 3820.
- (5) Jarvis, M. C. *Carbohydr. Res.* **1994**, *259*, 311.
- (6) Veregin, R. P.; Fyfe, C. A.; Marchessault, R. H.; Taylor, M. G. *Carbohydr. Res.* **1987**, *160*, 41.
- (7) Veregin, R. P.; Fyfe, C. A.; Marchessault, R. H.; Taylor, M. G. *Macromolecules* **1986**, *19*, 1030.
- (8) Gidley, M. J. *Macromolecules* **1989**, *22*, 351.
- (9) Zhang, P.; Klymchyov, A. N.; Brown, S.; Ellington, J. G.; Grandinetti, P. J. *Solid State Nucl. Magn. Reson.* **1988**, *12*, 221.
- (10) Chen, Y.-Y.; Luo, S.-Y.; Hung, S.-C.; Chan, S. I.; Tzou, D.-L. M. *Carbohydr. Res.* **2005**, *340*, 723.
- (11) Herzfeld, J.; Berger, A. E. *J. Chem. Phys.* **1980**, *73*, 6021.
- (12) Maricq, M. M.; Waugh, J. S. *J. Chem. Phys.* **1979**, *70*, 3300.
- (13) Crockford, C.; Geen, H.; Titman, J. J. *J. Chem. Phys. Lett.* **2001**, *344*, 367.

- (14) Shao, L.; Crockford, C.; Geen, H.; Grasso, G.; Titman, J. *J. Magn. Reson.* **2004**, *167*, 75.
- (15) Shao, L.; Titman, J. *Prog. Nucl. Magn. Reson.* **2007**, *51*, 103.
- (16) Payne, M. C.; Teter, M. P.; Allen, D. C.; Arias, T. A.; Joannopoulos, J. D. *Rev. Mod. Phys.* **1992**, *64*, 1045.
- (17) Clark, S. J.; Segall, M. D.; Pickard, C. J.; Hasnip, P. J.; Probert, M. J.; Refson, K.; Payne, M. C. *Z. Kristallogr.* **2005**, *202*, 567.
- (18) Pickard, C. J.; Mauri, F. *Phys. Rev. B: Condens. Matter Mater. Phys.* **2001**, *63*, 245101.
- (19) Sherwood, M. H.; Alderman, D. W.; Grant, D. M. *J. Magn. Reson., Ser. A* **1993**, *104*, 132.
- (20) Yates, J. R.; Pham, T. N.; Pickard, C. J.; Mauri, F.; Amado, A. M.; Gil, A. M.; Brown, S. P. *J. Am. Chem. Soc.* **2005**, *127*, 10216.
- (21) Lesage, A.; Emsley, L. *J. Magn. Reson.* **2001**, *148*, 449.
- (22) Bak, M. J.; Rasmussen, T.; Nielsen, N. C. *J. Magn. Reson.* **2000**, *147*, 296.
- (23) Edén, M.; Levitt, M. H. *J. Magn. Reson.* **1998**, *132*, 220.
- (24) Perdew, J. P.; Burke, K.; Ernzerhof, M. *Phys. Rev. Lett.* **1996**, *77*, 3865.
- (25) Vanderbilt, D. *Phys. Rev. B* **1990**, *41*, 7892.
- (26) Troullier, N.; Martins, J. L. *Phys. Rev. B: Condens. Matter Mater. Phys.* **1991**, *43*, 1993.
- (27) Brown, G. M.; Levy, H. A. *Acta Crystallogr., Sect. B: Struct. Sci.* **1973**, *29*, 790.
- (28) Gress, M. E.; Jeffrey, G. A. *Acta Crystallogr., Sect. B: Struct. Sci.* **1977**, *33*, 2490.
- (29) Jeffrey, G. A.; Nanni, R. *Carbohydr. Res.* **1985**, *137*, 21.
- (30) Fletcher, D.; McMeeking, R.; Parkin, D. *J. Chem. Inf. Comput. Sci.* **1996**, *36*, 746.
- (31) Hanson, J. C.; Sieker, L. C.; Jensen, L. H. *Acta Crystallogr., Sect. B: Struct. Sci.* **1973**, *29*, 797.
- (32) Hynes, R. C.; Le Page, Y. *J. Appl. Cryst.* **1991**, *24*, 352.
- (33) Witter, R.; Hesse, S.; Sternberg, U. *J. Magn. Reson.* **2003**, *161*, 35.
- (34) Tycko, R.; Dabbagh, G.; Mirau, P.A. *J. Magn. Reson.* **1989**, *85*, 265.
- (35) Hodgkinson, P.; Emsley, L. *J. Chem. Phys.* **1997**, *107*, 4808.
- (36) Tonelli, A. E.; Schilling, F. C. *Acc. Chem. Res.* **1981**, *14*, 233.
- (37) Malkin, V. G.; Malkina, O. L.; Casida, M. E.; Saluhub, D. R. *J. Am. Chem. Soc.* **1994**, *116*, 5898.
- (38) Chesnut, D. B. *Chem. Phys. Lett.* **2003**, *380*, 251.
- (39) Gervais, C.; Dupree, R.; Pike, K. J.; Bonhomme, C.; Profeta, M.; Pickard, C. J.; Mauri, F. *J. Phys. Chem. A* **2005**, *109*, 6960.